Calibration of Operating Reserve Demand Curves Using a System Operation Simulator

Jacques Cartuyvels, Anthony Papavasiliou, *Senior Member, IEEE,*

Abstract—The objective of this paper is to analyse the trade-off between the cost of operation and system reliability resulting from different shapes of Operating Reserve Demand Curves under scarcity pricing. We implement a model of the short-term operation of Belgium and we validate it against historical realisations of operation. The model of short-term operation is implemented using 4 embedded optimization problems. The model allows us to quantify the trade-off between the lag and cost of mobilizing flexible resources versus the increased reliability that these resources ensure for system operation. We compare eight variants of operating reserve demand curves, and use them as the basis for supporting a recommendation to the Belgian regulatory authority for the implementation of scarcity pricing in Belgium.

Index Terms—Scarcity pricing, operating reserve demand curve, unit commitment, economic dispatch, balancing, automatic frequency restoration reserve, manual frequency restoration reserve.

I. INTRODUCTION

THE increased integration of renewable resources in power systems has led to a tension in electricity markets. On the one hand, it has increased the need for flexible assets by increasing the variability and unpredictability of supply in the system. On the other hand, it has decreased the remuneration of flexible assets by pushing them further down the merit order curve and by consequently depressing the real-time energy price. This paradox raises concerns about the adequate remuneration of flexible resources, where flexible resources should be understood as resources that can provide automatic and manual frequency restoration reserves with a full activation times of five to fifteen minutes[1]. *Scarcity pricing* is a mechanism that has been considered as a possible remedy to the aforementioned lack of adequate incentives for investing in flexible assets.

Scarcity pricing is a mechanism for better remunerating energy and reserve in periods of scarcity. It relies on an *operating reserve demand curve* (ORDC) that introduces price elasticity in the procurement of reserve in the real-time market. Scarcity pricing mitigates the missing money problem by uplifting the real-time price for energy during periods of scarcity. Early references to this mechanism are found in Stoft in [1] and the theory was formally anchored to the *loss of load*

J. Cartuyvels is with the Center for Operations Research and Econometrics at UCLouvain, Louvain la Neuve, 1348, Belgium, e-mail: jacques.cartuyvels@uclouvain.be.

A. Papavasiliou is with UCLouvain.

[1]Such resources include, for instance, demand response, storage, combined cycle gas turbines and emergency generators.

probability (LOLP) and *value of loss load* (VOLL) by Hogan in [2] and [3].

Scarcity pricing based on operating reserve demand curves has commonly been associated with US markets, and the adaptation to European market design requires the introduction of EU-specific terminology. The real-time market and reserve are referred to as the balancing market and balancing capacity in Europe, respectively. We consider automatic and manual frequency restoration reserve (*aFRR* and *mFRR* respectively) in this paper. aFRR is driven by an automatic controller and can react within a few seconds in order to restore frequency deviations. It can thus be considered as synchronised reserve. The full activation time of aFRR is typically five minutes. mFRR is manually activated in order to cope with more significant system disturbances, including contingencies. These resources need to be fully available within 15 minutes and bear similarities to contingency reserve.

Scarcity pricing has been increasingly considered for implementation by a number of US ISOs, such as ERCOT and PJM. In these markets, there has been a transition from an ORDC with a fixed reserve requirement to a downward sloping ORDC based on the VOLL and LOLP [4]. ISO-NE and MISO are also considering this transition, following the recommendation of their respective market monitors.

TSOs and regulators in Europe have also considered variations of scarcity pricing mechanisms. A Reserve Scarcity Pricing function based on the VOLL and the amount of leftover reserve based on hour-ahead measurements is implemented in Great Britain [5]. Ireland has also implemented a scarcity pricing mechanism, nevertheless it is not based on ORDC and LOLP but rather triggered by stress conditions in the system [6], [7]. Poland is planning to implement a scarcity pricing scheme by the first half of 2023. The Polish scheme would be based on an ORDC based on VOLL and LOLP, and would remunerate non-contracted but available balancing capacity [8].

In Belgium, a number of studies have been performed on behalf of the Belgian regulatory authority for energy, in order to assess the potential of scarcity pricing based on ORDC [9], [10]. In more recent work, [11] investigates the adaptation of the mechanism, which has been inspired by US-style two-settlement systems, to European market design. A central measure proposed in this work is the implementation of a real-time market for reserve capacity [12], [13]. The current work advances this research effort for analyzing the implementation of the mechanism in EU markets by focusing on the calibration of the operating reserve demand curves. This is a key design parameter of the mechanism.

The calibration of ORDCs has largely been restricted to *open-loop* analyses in the existing literature [14], [15]. The Belgian TSO, ELIA, studies scarcity pricing in Belgium in [15]. Zarnikau [14] analyses the impact of scaling ORDCs horizontally, as well as the effect of the ORDC on the real-time market price and investment incentives for natural-gas-fired generation in the Texas electricity market.

Reference [14] highlights the influence of the shape of ORDC on the price and how the calibration of the ORDC can affect the remuneration of different technologies through its effect on prices. Nevertheless, the open-loop approach proposed in the paper is not able to capture the dispatch and commitment incentives created by different calibrations of the ORDC. This shortcoming of open-loop analyses motivates our proposal for a nested modelling approach for simulating the short-term operation of the system and for modelling the interplay between reserve prices and operational efficiency.

Our simulator models the operation of a perfectly coordinated system, where a centralized optimization model commits and dispatches resources in a coordinated fashion. Uncertainty is assumed to stem from the actual load that needs to be served by the system. The sequential optimization of system scheduling aims at replicating the real-time controllability of the different assets present in the system, with a specific focus on quantifying the interplay between lags in decision making and the revelation of uncertain information in the system. This allows us to quantify the fundamental tradeoff that ORDCs aim at balancing: incurring non-negligible fixed costs for committing flexible resources that can allow the system to operate reliably in real time, versus running the risk of not covering imbalances fully.

The nested modelling of system operation also appears in [16] and [17], albeit less detailed. Nested models also appear in other contexts in [18] and [19]. We proceed to discuss the relation of these publications to our work.

Zhou and Botterud [16] develop their model in order to analyze an ORDC which is based on the loss of load probability, and which accounts for the uncertainty caused by wind and load forecast errors, as well as generation contingencies. Lavin et al. [17] introduce an LOLP which is a function of the ambient temperature, in order to represent the higher probability of forced generator outages under extreme temperature conditions. Those models use short-term system operation simulators in order to compare different ORDC schemes. Nevertheless, these publications mostly leave aside the aspect of calibrating the ORDC. More specifically, the results of Zhou and Botterud [16] and Lavin et al. [17] are limited by the hourly temporal granularity of their model, as they cannot quantify the tradeoff between short-term dispatch adjustments and the lagged activation of reserves. The increased precision of our model remedies this shortcoming, and advances the state of the art by assessing more faithfully the interplay between costs and lags versus reliability of operation for different calibrations of ORDC.

In this sense, the precision of our model is closer to the Smart-ISO model of Simao and Powell [18]. The model of [18] is inspired by ISO practices and it is used in order to asses the reliability of the PJM system under different levels of wind power integration. We can also draw similarities with the model of Bakirtzis and al. in [19] where the authors propose a number of short-term operating models in order to cope with the increased uncertainties of power system operations. Note, however, that neither of the aforementioned papers is focused on the question of the calibration of ORDCs.

The main contributions of this paper are thus twofold. We introduce of a quantitatively sound methodology for calibrating ORDCs which anchors the calibration of an ORDC to a closed-loop simulation model and examines three specific design criteria for ORDCs that emerge in a realistic implementation of the mechanism. Moreover, we implement detailed system operation models for quantifying the tradeoff between incurring fixed costs for committing flexible resources and allowing the system to operate reliably versus running the risk of shedding load.

In addition to the methodological novelty of our analysis, there is an important institutional dimension to our work. The current modeling effort is contributing directly to the implementation of a scarcity pricing mechanism in the Belgian electricity market. The results of the analysis constitute the basis for our recommendation to the Belgian regulatory authority for the possible implementation of scarcity pricing in Belgium in the short to medium term.

The paper is structured as follows. Section II summarizes the principles of scarcity pricing, with a specific focus on certain dilemmas pertaining to the calibration of ORDCs. Section III presents the short-term operating model that we have developed in order to support the calibration of an ORDC. Our case study of the Belgian market is presented in section IV. The results of the case study are presented and analysed in section V. Finally, we conclude and discuss future research perspectives in section VI.

II. SCARCITY PRICING AND ORDC

The argument that rationalizes the implementation of scarcity pricing with ORDCs based on LOLP and VOLL relies on the intrinsic stochasticity of an economic dispatch and in its deterministic approximation [3]. In this setting, the value of an additional MW of balancing capacity is linked to the value of the improved reliability that it provides to the system by reducing the likelihood of load shedding. This marginal value is characterised by Hogan in [3] as a function of the value of lost load ($VOLL$), the loss of load probability ($LOLP(\cdot)$) given the level of reserve in the system (r) and the marginal cost of the marginal unit in the system ($\widehat{MC}$):

$$V^R(r) = (VOLL - \widehat{MC}) \cdot LOLP(r) \qquad (1)$$

The most complete integration of scarcity pricing based on ORDC to electricity market operations would correspond to the co-optimization of reserve and energy in real time. An ORDC based on (1) would then be the explicit demand curve for reserve and would be inserted in the multi-product auction that trades energy and reserve simultaneously. Co-optimized markets would then produce one price for each product: (i) a reserve price for the available reserve and (ii) an energy price for the energy traded. Note that, in the absence of binding

ramp constraints, the price of energy will be coupled to the price of reserve in order to ensure an equivalence between the marginal profit on the energy and reserve market for a marginal generator that supplies both reserve and energy.

In the absence of a co-optimization of energy and reserves, we could use the expression of Eq. (1) to compute *adders* based on the amount of reserve that is available in real time, as measured by system telemetry. This adder reflects the level of stress in the system, and would correspond to the price of reserve. The coupling between reserve and energy prices would then be implemented by adding this adder as a price component to the real-time energy price in the absence of co-optimization (the balancing energy price in EU nomenclature).

A. Multiple Reserve Products

Formula (1) has been generalized by Hogan in [20] to the case of multiple reserve products of different quality. The quality of reserve refers to the delivery time that is required for this specific reserve product to be fully available, which in EU jargon is referred to as *full activation time*. This generalization is based on the split of a real-time dispatch interval two parts. In the first part of the interval, it is assumed that only high-quality resources can respond, whereas in the second part of the interval, all reserve types are assumed to be able to respond. We consider the full interval as an imbalance interval.

In the EU, the reference duration for an imbalance interval is 15 minutes and [21] suggests the following split of the real-time dispatch based on the products that have been historically available in the EU balancing market. The first part of the interval would last 7.5 minutes and imbalances would be resolved by balancing capacity that can be fully activated in no longer than 7.5 minutes (which corresponds in our analysis to aFRR capacity[2]). The second part of the interval would also last for 7.5 minutes. In this time interval, imbalances would be resolved by balancing capacity that can be fully activated in 15 minutes (which correspond in our analysis to mFRR capacity).

Based on this split of an imbalance interval, the authors in [21] suggest the introduction of two ORDCs: (i) a 7.5-minute ORDC (eq. (2)) for the first part of the interval and (ii) the 15-minute ORDC (eq. (3)) for the second part of the interval:

$$V_{7.5}^R(r_{7.5}) = \frac{1}{2} \cdot (VOLL - \widehat{MC}) \cdot LOLP_{7.5}(r_{7.5}) \quad (2)$$

$$V_{15}^R(r_{15}) = \frac{1}{2} \cdot (VOLL - \widehat{MC}) \cdot LOLP_{15}(r_{15}) \quad (3)$$

Here, $LOLP_x(\cdot)$ corresponds to the loss of load probability after x minutes, and r_x is the amount of reserve that can be activated within x minutes. The loss of load probability after x minutes is described in equation (4) and represents the probability of the imbalance after x minutes exceeding the balancing capacity that can be made available in x minutes:

$$LOLP_x(r_x) = \mathbb{P}(imb_x \geq r_x) \text{ with } imb_x \sim \mathcal{N}(\mu_x, \sigma_x^2). \quad (4)$$

The imbalance is assumed to be drawn from a normal distribution with mean μ_x and standard deviation σ_x. These parameters can be estimated from the historical system imbalance. They are computed per 4-hour block and per season, in order to account for seasonality.

The settlement in a co-optimized market can be understood by analysing the following model in a convex setting. Assuming a benefit function for demand ($B(\cdot)$) and a constant production cost for generator $g \in \mathcal{G}$ (C_g), where $\mathcal{G}$ is the set of generators in the system, our goal is to maximize the welfare of the system as a function of the demand (d), reserve available after 7.5 and 15 minutes ($r_{7.5}$ and r_{15})[3] and the production (p_g) and supply of fast and slow reserve (r_g^F and r_g^S) for every generator g:

$$\max_{\substack{d,p,r^S, \\ r^F, r_{7.5}, r_{15}}} B(d) - \sum_g C_g \cdot p_g + \int_0^{r_{7.5}} V_{7.5}^R(x)dx + \int_0^{r_{15}} V_{15}^R(x)dx, \quad (5)$$

The co-optimization must obey the market clearing constraint for energy and fast and slow reserve (the associated dual variables are provided in brackets):

$$(\lambda): \quad d = \sum_g p_g, \quad (6)$$

$$(\lambda^{7.5}): \quad r_{7.5} \leq \sum_g r_g^F, \quad (7)$$

$$(\lambda^{15}): \quad r_{15} \leq \sum_g (r_g^F + r_g^S), \quad (8)$$

The operating constraints of generator g are characterised by the set $\mathcal{X}_g$:

$$(p_g, r_g^S, r_g^F) \in \mathcal{X}_g. \quad (9)$$

It is worth noting that the fast reserve supplied by the generators is eligible not only for the pool of reserve available after 7.5 minutes (Eq. (7)) but also for the pool of reserve available after 15 minutes (Eq. (8)).

The profit maximization problem faced by a generator g can be obtained by first relaxing the market clearing constraints of the co-optimization model (Eqs. (6)-(8)):

$$\max_{\substack{d,p,r^S, \\ r^F, r_{7.5}, r_{15}}} B(d) - \sum_g C_g \cdot p_g + \int_0^{r_{7.5}} V_{7.5}^R(x)dx + \int_0^{r_{15}} V_{15}^R(x)dx$$

$$+ \lambda \cdot (\sum_g p_g - d) + \lambda^{7.5} \cdot (\sum_g r_g^F - r_{7.5})$$

$$+ \lambda^{15} \cdot (\sum_g r_g^F + \sum_g r_g^S - r_{15}) \quad (10)$$

$$(s.t.) \quad (p_g, r_g^S, r_g^F) \in \mathcal{X}_g, \quad \forall g \in \mathcal{G}, \quad (11)$$

and then decomposing the relaxed problem by $g \in G$:

$$\max_{p_g, r_g^S, r_g^F} p_g \cdot (\lambda - C_g) + r_g^F \cdot (\lambda^{15} + \lambda^{7.5}) + r_g^S \cdot \lambda^{15} \quad (12)$$

$$(s.t) \quad (p_g, r_g^S, r_g^F) \in \mathcal{X}_g. \quad (13)$$

---

[2]Note that, even though the full activation time of aFRR that is envisioned in the pan-European platform PICASSO for the activation of aFRR capacity is 5 minutes, the current analysis is performed for the Belgian system whose aFRR has been required to be fully activated in 7.5 minutes in the past [22].

[3]The value of r_{15} would be computed in practice ex post, based on telemetry measurements. In case the resolution of telemetry data is 15 minutes, it would be necessary to assume a pre-defined availability of different resources for 7.5 minutes, which is the case in our present study.

From the generator point of view, $\lambda, \lambda^{7.5}$ and λ^{15} are exogenous parameters representing respectively the price of energy and of reserve for the first and second interval of an imbalance period. From the system operator point of view, these prices are can be obtained by solving the initial co-optimization problem.

The prices of reserve for the first and second interval, $\lambda^{7.5}$ and λ^{15}, are set by the ORDCs. This is demonstrated by the KKT conditions of the initial co-optimization problem relative to the complementarity constraints implicating variables $r_{7.5}$ and r_{15} in (14) and (15):

$$0 \leq r_{7.5} \perp \lambda^{7.5} - V_{7.5}^R(r_{7.5}) \geq 0 \qquad (14)$$

$$0 \leq r_{15} \perp \lambda^{15} - V_{15}^R(r_{15}) \geq 0 \qquad (15)$$

Generators are then remunerated according to (12) under co-optimization.

- Balancing capacity that can be made available in 7.5 minutes is remunerated with the *fast reserve price*:

$$\lambda^F = V_{7.5}^R(r_{7.5}) + V_{15}^R(r_{15}). \qquad (16)$$

- Balancing capacity that can be made available in 15 minutes is remunerated with the *slow reserve price*:

$$\lambda^S = V_{15}^R(r_{15}). \qquad (17)$$

- Energy is remunerated in real time, with the energy price, λ.

A notable challenge of integrating scarcity pricing in the EU and certain past US markets is the lack of co-optimization in the European market. Without co-optimization, a system operator cannot rely anymore on the dual variables of the co-optimization problem in order to characterize the prices and needs to resort to approximations. In the past, ERCOT has used adders as proxies to couple the reserve and energy prices, although the evolution of the ERCOT design is towards a co-optimization model [23].

In the spirit of the original ERCOT design, [21] suggests to introduce 3 adders in order to approximate pricing under co-optimization. The *fast adder* and *slow adder* would be equal to the fast and slow reserve price and would remunerate balancing capacity that can be made available in 7.5 and 15 minutes. The *energy adder* would be equal to the fast adder and would be added to the real-time balancing price for remunerating energy.

Assuming that the energy adder is equal to the fast adder is an approximation that presumes non-binding ramp constraints. The reader is referred to the supplement of [11] for a more detailed discussion about this approximation. The explanation can be summarized as follows. The price of energy is fixed by the KKT conditions of the initial co-optimization problem relative to the generation variables p_g, r_g^F and r_g^S. Depending on the which constraints of the model are binding, the energy price may be offset by a constant with respect to the fast adder, the slow adder, or neither.

B. Variants of ORDC

Eqs. (2) and (3) depend on a number of design parameters. Different variants of ORDCs can be produced depending on these assumptions. In this paper, we consider the following design parameters, which have been discussed in the context of the implementation of scarcity pricing in Belgium: (i) different values for VOLL, (ii) whether the argument of the LOLP operator is the reserve capacity remaining before or after the activation of reserve and (iii) whether imbalance increments within an imbalance interval are assumed to be correlated or not.

1) VOLL at 8300 €/MWh versus 13500 €/MWh: The Belgian federal planning bureau has estimated the Belgian VOLL at 8300 €/MWh in [24]. This value has been used as the reference value of the VOLL in [21]. The value of 13500 €/MWh has also been suggested because it represents the current bidding limit of the imbalance price [25] and as such the market players' assumed highest VOLL.

2) Pre- versus Post-Activation: Reference [11] points out that the pre- and post-activation variants correspond to different interpretations of what making a certain quantity of reserve available in real time would mean in terms of system operator expectations. The pre-activation interpretation means that 1 MW of reserve implies that a resource has been afforded time to recover from its balancing dispatch during the previous imbalance interval. The post-activation interpretation means that the resource is prepared to offer 1 MW even if it has not been afforded time to return to its originally scheduled setpoint. The effect of the assumption is found to be significant in the context of the stochastic equilibrium formulation presented in [11]. As the time step of the real-time / balancing market becomes shorter (5 minutes currently in the US, and 15 minutes in Europe), the distinction becomes less relevant.

If the post-activation reserve capacity margin is denoted as r, then the pre-activation margin is $r - imb$, with imb being the difference between the scheduled and actual demand. This allows us to value balancing capacity at the beginning of an interval before absorbing the imbalance.

3) Independent versus Correlated Imbalance Increments: When splitting an imbalance periods into two intervals, the full imbalance that needs to be covered also has to be split into two *imbalance increments*. Each interval is then responsible for causing one of the two imbalance increments. The assumption then is on how imbalance increments correlate in these two separate time steps. On the one extreme, we can assume correlated increments which implies that the total imbalance over both stages evolves linearly from the beginning to the end of the interval. On the other extreme, the assumption of independent imbalances implies that the total imbalance over both stages is the sum of two independently distributed imbalance increments occurring at stages 1 and 2 respectively.

The distinction affects the implied standard deviation of the imbalance that is used in the 7.5-minute version of Eq. (4). Given σ and μ, the standard deviation and mean of the 15-minute imbalance, the standard deviation of the 7.5-minute increments is either $\sigma/\sqrt{2}$ if the increments are independent, or $\sigma/2$ if the increments are perfectly correlated. The mean of both the independent and correlated 7.5-minute increments is $\mu/2$.

III. SIMULATOR FOR SHORT-TERM OPERATION

The short-term operating model that we develop for the purpose of our analysis is composed of 4 embedded optimization problems that are solved in sequence throughout the day. Simulations begin in the day ahead by scheduling inelastic production, and unfold in intraday and real time by solving a sequence of unit commitment and economic dispatch problems with different scheduling windows. Each problem is employed for the commitment and / or dispatch of specific types of plants, depending on their response speed.

Particular care is given to (i) the operational constraints of the individually modelled generation plants, (ii) the revelation of real-time uncertainty and the scheduling of the system based on forecast information, and (iii) the effect of each decision-making stage on subsequent optimization problems.

Depending on the characteristics of an asset, its commitment plan and dispatch decisions will be obtained by different optimization problems. Assets can be partitioned into 3 broad categories, based on their real-time controllability.

1) **DA scheduled generators** cannot modify their planned day-ahead dispatch. This might be due to the inflexibility of the technology, or a link between electricity production and other processes, such as heating. The electricity production of these generators is typically determined in forward processes, and these units are not participating in a balancing market.

2) **Fast balancing capacity generators** require a non-negligible lag to start up (between 1 and 3 hours) but are very reactive once committed. CCGT generators constitute the bulk of this category.

3) **Slow balancing capacity generators** include all emergency generators and demand response resources. These generators are typically costly to start up, but can be activated in a very short time, in order to free up some of the fast balancing capacity[4].

The 4 dispatch and commitment models that we develop optimize different subsets of the aforementioned assets. The dependencies are described hereunder. The sequencing of the models in the simulator is indicated in Fig. 1.

- **The day-ahead unit commitment (DA-UC) model** is used for scheduling the inelastic production that will not vary in real time relative to its day-ahead set-point. The model is launched once, before the beginning of the day, with a scheduling horizon of 72 hours. The model assumes a fixed initial dispatch of units for the day, which will be identical for every variant of ORDC that is tested in our analysis. The parameters of the simulation include the day-ahead load forecast, as well as settings that determine the reactivity and availability of the generation pool. This problem also determines the hydro storage target for the real-time models. The system is allowed to deviate from this target in order to address balancing issues, but such deviations are penalized.
- **The intermediate rolling-window unit commitment (Inter-RUC)** is solved every six hours over a 24-hour

scheduling window. The Inter-RUC determines the commitment of CCGT plants for the next 6 hours until the next Inter-RUC is launched. This process thus proxies intraday market adjustments. It is costly to keep CCGT plants online, therefore an optimal scheduling of these plants requires a significant scheduling window.

- **The pre-real-time rolling-window unit commitment (PRT-RUC)** determines the commitment of emergency generators. The model is launched every 15 minutes over a 1-hour scheduling window.
- **The real-time economic dispatch (RT-ED)** dispatches the generators that are committed in the previous optimization problems.

A. Generic Unit Commitment Problem

All the optimization problems are based on a standard unit commitment problem that aims at minimizing the total cost of the system under a series of constraints for both classical and pumped hydro generation.

1) Sets, Variables and Parameters: We define $\mathcal{T} = \{t_1, t_2, \ldots t_T\}$ as the scheduling window for a problem, D as the demand, $\mathcal{G} = \{1, 2, \ldots N\}$ as the set of generators and $\mathcal{S} = \{7.5, 15\}$ as the type of ORDC considered in this analysis. Let us also denote V_{it}^R as the marginal benefit function of reserve type i at period t. The segments of the ORDC are obtained by approximating (2) and (3) with a stepwise constant function[5].

The set of decisions concerning a generator g at period t is characterized by the point $x_{g,t} = (p_{g,t}, r_{g,t}^F, r_{g,t}^S, r_{g,t}^{NS,F}, r_{g,t}^{NS,S}, u_{g,t}, v_{g,t}, w_{g,t}, s_{g,t})$. This vector is the concatenation of the production, fast reserve, slow reserve, fast non-spinning reserve, slow non-spinning reserve and binary variables for the commitment, activation, shut-down and start-up of generator g at time t. The vector $x_{g,t}$ belongs to the set $X = \mathbb{R}_+^5 \times \mathbb{B}^4$.

Each generator g is characterized by its technical parameters $P_g^+, P_g^-, R_g, R_g^{NS,F}, R_g^{NS,S}, UT_g, DT_g$ and SU_g which are respectively the maximum and minimum production limit, the ramp rate, the limit for fast and slow non-spinning reserve, the minimum up time and down time, the start-up time of the unit, and its cost function $C_g : X \to \mathbb{R}$. The cost function includes the fixed cost of keeping a generator online, the start-up cost of starting it up, and the fuel cost with variable heat-rate.

We represent demand for energy and reserve using the vector $m_t = (z_t, r_t^{7.5}, r_t^{15})$. This tuple consists of the shortage in energy and the system supply for reserve for both the first and second half of an imbalance interval interval for period t. The hydro vector $h_t = (p_t^H, d_t^H, e_t^H, r_t^{H,F}, r_t^{H,S}, u_t^H)$ represents the production, consumption, energy stored, fast and slow reserve supplied by pumped hydro, and the pumping mode of a pumped hydro unit for period t. Note that $m_t \in \mathbb{R}_+^3$ and $h_t \in \mathbb{R}_+^5 \times \mathbb{B}^1$.

We further introduce the notation t_- to characterize the period preceding period t.

---

[4]Fast and slow balancing capacity resemble spinning and non-spinning reserve, respectively, in US terminology.

[5]A method to approximate (1) by a stepwise constant function is proposed in [16].
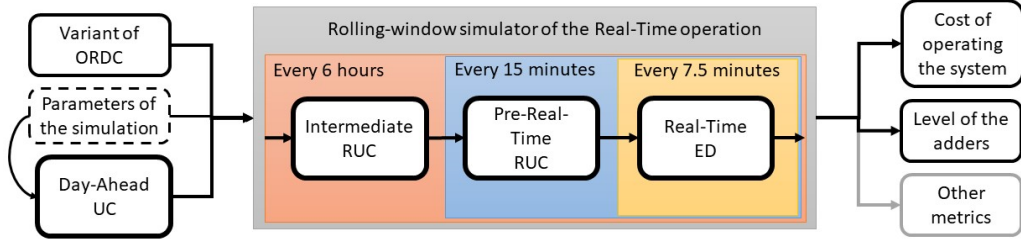
Fig. 1. Sequence of models in our simulator of short-term operation.

2) Objective Function: The system operator aims at minimizing the sum of the production cost and shortage cost minus the benefit from reserve:

$$\min_{\substack{x_{g,t}, \\ m_t,h_t}} \sum_{t\in\mathcal{T}} \Big(\sum_{g\in\mathcal{G}} C_g(x_{g,t}) + VOLL \cdot z_t - \sum_{i\in\mathcal{S}} \int_0^{r_t^i} V_{it}^R(x)dx \Big).$$

$$(18)$$

The cost of shedding load is valued at the VOLL.

3) Market Clearing Constraints:

$$D_t = \sum_{g\in\mathcal{G}} p_{g,t} + p_t^H - d_t^H + z_t \qquad \forall t \in \mathcal{T} \quad (19)$$

$$r_t^{7.5} \le \sum_{g\in\mathcal{G}_D} r_{g,t}^F + r_{g,t}^{NS,F} + r_t^{H,F} \qquad \forall t \in \mathcal{T} \quad (20)$$

$$r_t^{15} \le \sum_{g\in\mathcal{G}_D} r_{g,t}^S + r_{g,t}^{NS,S} + r_t^{H,S} + r_t^{7.5} \quad \forall t \in \mathcal{T} \quad (21)$$

Constraint (19) ensures that the market is balanced at all times, and constraints (20) and (21) define the market clearing conditions for fast and slow reserve. Reserve can be sourced from online generators (spinning reserve), from offline generators (non-spinning reserve) or from hydro (hydro reserve).

4) Generation Constraints:

$$r_{g,t}^F \le R_g \cdot 7.5 \qquad \forall g \in G, \forall t \in \mathcal{T} \quad (22)$$

$$r_{g,t}^S \le R_g \cdot 15 \qquad \forall g \in G, \forall t \in \mathcal{T} \quad (23)$$

$$p_{g,t} + r_{g,t}^F + r_{g,t}^S \le P_g^+ \cdot u_{g,t} \quad \forall g \in G, \forall t \in \mathcal{T} \quad (24)$$

$$p_{g,t} \ge P_g^- \cdot u_{g,t} \qquad \forall g \in G, \forall t \in \mathcal{T} \quad (25)$$

Eqs. (22) to (25) represent the ramp constraints of fast and slow reserve and the maximum and minimum technical production limits of a unit.

5) Non-Spinning Reserve Constraints:

$$r_{g,t}^{NS,F} \le R_g^{NS,F} \cdot (1 - u_{g,t}) \qquad \forall g \in G, \forall t \in \mathcal{T} \quad (26)$$

$$r_{g,t}^{NS,F} + r_{g,t}^{NS,S} \le R_g^{NS,S} \cdot (1 - u_{g,t}) \quad \forall g \in G, \forall t \in \mathcal{T} \quad (27)$$

Eqs. (26) and (27) limit the supply of non-spinning reserve from offline generators. Most of the generators cannot provide non-spinning reserve and their parameters $R_g^{NS,F}$ and $R_g^{NS,S}$ are equal to 0.

6) Transition Constraints:

$$p_{g,t} - p_{g,t_-} \le R_g \cdot T \cdot (1 - v_{g,t}) + P_g^- \cdot v_{g,t} \quad \forall g \in G, \forall t \in \mathcal{T}$$
$$(28)$$

$$v_{g,t} + u_{g,t_-} - u_{g,t} - w_{g,t} = 0 \qquad \forall g \in G, \forall t \in \mathcal{T}$$
$$(29)$$

The transition constraints (28) and (29) represent the ramp constraint for production and the commitment transition constraint. The production ramp constraint has two possible modes: one for normal operation and one for activation. The parameter T is the number of minutes of one period in a specific problem. For example, $T = 60$ for the DA-UC problem.

7) Operating Constraints:

$$w_{g,t} + \sum_{t'=max(t_0,t-UT_g+1)}^{t} v_{g,t'} \le 1 \qquad \forall g \in G, \forall t \in \mathcal{T} \quad (30)$$

$$v_{g,t} + \sum_{t'=max(t_0,t-DT_g+1)}^{t} w_{g,t'} \le 1 \qquad \forall g \in G, \forall t \in \mathcal{T} \quad (31)$$

$$SU_g \cdot v_{g,t} - \sum_{t'=max(t_0,t-SU_g+1)}^{t-1} s_{g,t'} \le 0 \quad \forall g \in G, \forall t \in \mathcal{T} \quad (32)$$

The operating constraints (30), (31) and (32) represent the minimum down time, minimum up time and start-up time of assets. Similarly as for T, UT, DT and SU are adapted to the granularity of the problem under consideration.

8) Hydro Generation Constraints:

$$d_t^H \le D_H^{Max} \cdot u_t^H \qquad \forall t \in \mathcal{T} \quad (33)$$

$$e_t^H \le E_H^{Max} \qquad \forall t \in \mathcal{T} \quad (34)$$

$$p_t^H + r_t^{H,F} + r_t^{H,S} \le P_H^{Max} \cdot (1 - u_t^H) \quad \forall t \in \mathcal{T} \quad (35)$$

$$p_t^H + r_t^{H,F} + r_t^{H,S} \le e_t^H \qquad \forall t \in \mathcal{T} \quad (36)$$

$$e_t^H = e_{t_-}^H - \frac{60}{T}(p_{t_-}^H + d_{t_-}^H \cdot \eta) \qquad \forall t \in \mathcal{T} \quad (37)$$

The pumped hydro generation constraints restrict the maximum hydro consumption, energy stored and hydro production in constraints (33) - (35) with the pump hydro characteristics D_H^{Max}, E_H^{Max} and P_H^{Max}. Note that a unit is either pumping or producing, as a function of the pumping mode u_t^H. Eq. (36) restricts the hydro reserve to the total stored energy. Constraint (37) describes the evolution of energy stored in the reservoir as a function of pumping and production decisions in the previous period, as well as the efficiency of the plant.

B. Modifications for the Intraday and Real-Time Problems

The intraday problem (Inter-RUC) and real-time problems (PRT-RUC and RT-ED) extend the standard unit commitment problem described previously to account for the day-ahead schedule and the particularities of the balancing market.

1) Day-ahead Constraints:

$$r_{g,t}^F = 0 \qquad \forall g \in \mathcal{G}_I, \forall t \in \mathcal{T} \tag{38}$$

$$r_{g,t}^S = 0 \qquad \forall g \in \mathcal{G}_I, \forall t \in \mathcal{T} \tag{39}$$

$$p_{g,t} = p_{g,t}^{DA,*} \qquad \forall g \in \mathcal{G}_I, \forall t \in \mathcal{T} \tag{40}$$

Given the set $\mathcal{G}_I$ representing the DA-scheduled generators, constraints (38) and (39) restrict their ability to supply reserve. Constraint (40) characterizes their real-time inflexibility by equalizing the real-time production to the scheduled day-ahead production $p_{g,t}^{DA,*}$.

2) Status Constraints: The commitment decisions of previous optimization models are enforced by this set of constraints. We introduce the notation $\mathcal{S}_{U,t}$, $\mathcal{S}_{S,t}$, $\mathcal{S}_{A,t}$ and $\mathcal{S}_{F,t}$ to represent the set of generators that are unavailable, in the start-up process, activated or free in period t[6].

$$u_{g,t} = 0 \qquad \forall t \in \mathcal{T}, \forall g \in \mathcal{S}_{U,t} \cup \mathcal{S}_{S,t} \tag{41}$$

$$u_{g,t} = 1 \qquad \forall t \in \mathcal{T}, \forall g \in \mathcal{S}_{A,t} \tag{42}$$

$$s_{g,t} = 1 \qquad \forall t \in \mathcal{T}, \forall g \in \mathcal{S}_{S,t} \tag{43}$$

Constraints (41) and (42) imply that a generator is either off ($u_{g,t} = 0$) or on ($u_{g,t} = 1$) because of the minimum down time and minimum up time constraints of previous optimization problems. Similarly, Eq. (43) enforces the start-up variables dictated by a start-up decision in a previous problem and its start-up time.

3) Hydro-Deviation Constraints: The opportunity cost of hydro in real time is modelled by a hydro storage target $e_t^{DA,*}$ and the variable q_t representing the deviation from that target:

$$q_t \geq e_t^{DA,*} - e_t^H \qquad \forall t \in \mathcal{T} \tag{44}$$

$$q_t \geq e_t^H - e_t^{DA,*} \qquad \forall t \in \mathcal{T} \tag{45}$$

$$q_t \geq 0 \qquad \forall t \in \mathcal{T} \tag{46}$$

The term $\sum_{t \in \mathcal{T}} \int_0^{q_t} HD(q) dq$ is subtracted from the objective function of the real-time problem in order to penalize deviations.

4) Start-Up Constraints: The scheduling window for the pre-real-time problem is defined as $\mathcal{T} = \{t_{0,0}, t_{0,1}, t_1, \ldots, t_{w-1}\}$. It represents two 7.5-minute periods ($t_{0,0}$ and $t_{0,1}$) and $w - 1$ 15-minute periods. This window plans over $w \cdots 15$ minutes. The first period is split, in order to account for the start-up profile of emergency generators and how much of their generation is available after 7.5 minutes. Given the initial position of a generator p_g^0, the initial transition constraint of equation (28) needs to be reformulated:

$$p_{g,t_{0,0}} - p_g^0 \leq R_g \cdot 7.5 \cdot (1 - v_{g,t}) + R_g^{SU,0} \cdot v_{g,t} \tag{47}$$
$$\forall g \in G, \forall t \in \mathcal{T}$$

$$p_{g,t_{0,1}} - p_{g,0,1} \leq R_g \cdot 7.5 \cdot (1 - v_{g,t}) + R_g^{SU,1} \cdot v_{g,t} \tag{48}$$
$$\forall g \in G, \forall t \in \mathcal{T}$$

$$u_{g,t_{0,0}} = u_{g,t_{0,1}} \quad \forall g \in G, \forall t \in \mathcal{T} \tag{49}$$

$$v_{g,t_{0,0}} = v_{g,t_{0,1}} \quad \forall g \in G, \forall t \in \mathcal{T} \tag{50}$$

---

[6]No generator can be in two sets at the same time and all generators must be in a set at every period t.

The start-up constraints (47) and (48) ensure that generators comply with their start-up profile. This start-up profile is characterized by the maximum production 7.5 minutes and 15 minutes after activation ($R_g^{SU,0}$ and $R_g^{SU,1}$). The start-up ramp profile is similar to the limit on non-spinning reserve for emergency generators and demand response.

Note that the two 7.5-minute dispatch periods only account for one 15-minute commitment period (Eqs. (49)-(50)).

5) Economic Dispatch Constraints: The real-time economic dispatch is similar to the first and second period of the pre-real-time unit commitment except that all the generators are either activated, unavailable or in start-up. No commitment decision is taken in this problem.

IV. MODEL VALIDATION AGAINST HISTORICAL DATA

A. Case Study

The investigation is performed on the Belgian power system with the historical load of 2018.

1) Generation pool: The generation pool modelled in the simulator includes all the controllable assets of Belgium and is mainly based on the database of installed capacity by unit, which is publicly available on the Elia website [26].

In addition to classical thermal generators, this pool includes demand response, pumped-hydro and some foreign balancing capacity[7]. Demand response varies from month to month and is extracted from historical data. Foreign balancing capacity is set administratively to 50 MW.

The technical parameters relative to the operating constraints of the flexible generators are largely aligned with [27], except for the minimum production of emergency generators. We consider emergency generators and demand response as "all-or-nothing" generators.

2) Net Load: Net load is modelled as the power that must be served by flexible and controllable assets. It corresponds to the difference between grid load and renewable energy and imports / exports.

The data that we use for net load is obtained from ELIA [28] and the ENTSO-E transparency platform [29]. The data resolution of the ELIA website and ENTSO-E platform is respectively 15-minute and hourly.

3) Imbalance: The mean and standard deviation of the distribution of the imbalances used for the LOLP in (4) is obtained from the historical system imbalance recorded in [28]. For simulating 2018, we use the historical imbalance of the 3 preceding years. The full characterization of the mean and standard deviation of the system imbalance can be found in the electronic supplement.

B. Validation

We validate our model by assessing the quality of the forward position computed by the day-ahead unit commitment compared to the historical records of day-ahead positions. The validation is restricted to the day-ahead unit commitment because the co-optimization of reserve and energy in real time

---

[7]Demand response and foreign balancing capacity are referred to as *Non-CIPU generation* and *Inter-TSO* in the Belgian framework.

TABLE I
MEAN ERROR (ME), MEAN ABSOLUTE ERROR (MAE) AND ROOT MEAN SQUARED ERROR (RSME) BETWEEN THE HISTORICAL AND SIMULATED PRODUCTION PER TYPE OF FUEL FOR 2018 AND COMPARISON WITH THE ERRORS OF THE STUDY IN [9] FOR 2013.

		Gas	Hydro	Fuel	Nucl.	Other
ME	Simulator	-76.7	28.5	0.0	2.7	140.4
	1st Study	168.9	4.7			
MAE	Simulator	208.8	69.2	0.0	36.8	148.7
	1st Study	240.7	61.6			
RMSE	Simulator	267.7	113.7	1.0	116.2	176.9
	1st Study	309.9	119.3			

TABLE II
DECOMPOSITION OF THE MEAN TOTAL OPERATING COST OF EACH VARIANT IN MILLION € PER DAY.

			Total cost	Fuel cost	Fixed cost	Act. cost	Short. cost	Em. cost
8300	Pre-Acti.	Ind.	1.694	1.317	0.344	0.032	0.001	0.109
		Corr.	1.697	1.321	0.342	0.033	0.000	0.114
	Post-Act.	Ind.	1.691	1.316	0.343	0.032	0.000	0.107
		Corr.	1.694	1.318	0.343	0.033	0.000	0.110
13500	Pre-Act.	Ind.	1.688	1.304	0.352	0.031	0.000	0.101
		Corr.	1.687	1.302	0.350	0.033	0.002	0.097
	Post-Act.	Ind.	1.684	1.301	0.352	0.031	0.000	0.097
		Corr.	1.683	1.299	0.350	0.033	0.000	0.095

in our simulator is a closed-loop investigation that is expected to produce a different dispatch depending on the ORDC that we analyse.

The comparison is performed over the aggregated forecast production per type of fuel. There are five types of fuel, namely (i) nuclear, (ii) gas, (iii) hydro, (iv) liquid fuel and (v) other. We will mostly focus on gas and hydro production. Nuclear and other technologies are mainly driven by the maximum available output and liquid fuel is used as an emergency measure and is rarely scheduled in the day ahead.

The performance of the simulator is compared to that of [9]. The current work improves [9] by (i) refining and extending the generation pool, (ii) reducing the granularity of the dispatch, and (iii) proposing a more realistic modeling of the dispatch and commitment decisions. These enhancements allow us to analyse the tradeoff between the commitment of fast balancing capacity and the cost of operating the system with more realism. Table I details this comparison and demonstrates that the increased modeling detail does not come at the cost of accuracy in replicating past observations of the Belgian electricity system.

V. RESULTS AND ANALYSIS

The results presented in this section are obtained by simulating the historical demand of Belgium for 2018. The analysis is based on a reference scenario and on a sensitivity analysis on the availability of the slow balancing capacity for contributing towards satisfying the demand of the 7.5-minute ORDC.

Some of the slow balancing capacity is assumed to partly cover the demand of the 7.5 minute ORDC and [15] uncovers the importance of this assumption. We investigate further in this direction with the sensitivity analysis that is performed in section V-C. Note that the reference scenario assumes an availability of 28%.

Our analysis focuses on comparing the total operating cost of the different variants of ORDCs, and on analyzing the impact of these variants on the level of the scarcity adder. The comparison focuses largely on the level of conservatism of the variants. More conservative variants (value of lost load at 13500 €/MWh and / or independent 7.5-minute imbalance increments) are compared against less conservative variants (value of lost load at 8300 €/MWh and / or correlated 7.5-minute imbalance increments).

A. Cost Analysis of the Reference Scenario

The total cost of the variants is reported in Table II. The values reported here are obtained by adding the fuel cost, fixed cost, activation cost and shortage cost of the system, and do not include the cost of the price-inelastic generators, since the latter is identical across different scenarios. The last columns report the cost of emergency measures. The total cost varies from 1.697 M € per day to 1.683 M € per day. Thus, we find a difference of up to 14 k € per day between the different variants. This corresponds to a variation of up to 0.8% of the mean total flexible cost, which can be considered quite stable.

Despite the stability of the total cost, we can analyse the differences between the variants in order to better understand the impact of the ORDC on the commitment and dispatch decisions. Based on Table II, we can observe that more conservative variants are typically less costly. This trend is more accentuated for the variation of the VOLL, where the 13500 variants are consistently lower in cost than their 8300 counterpart. More conservative ORDCs tend to result in higher fixed costs, and this is balanced out by their lower fuel cost.

B. Price Analysis of the Reference Scenario

The values of the adders that result from the different variants under the reference scenario are presented in Table III. The fast adder varies from 2.7 €/MWh to 6.5 €/MWh and the slow adder from 0.15 €/MWh to 0.5 € per MWh. The adders generated by the different variants are thus more significantly dependent on the choice of ORDC than system cost. Two main observations can be highlighted from the table.

Firstly, conservative ORDCs (13500 variants and Independent variants) produce higher adders than their counterparts. Note that the most significant difference is caused by the distribution of the 7.5-minute imbalance increments, with the independent variants producing fast reserve adders that are approximately twice the value of their counterparts.

Secondly, correlated variants result in a higher slow reserve adder. This is driven by the fact that CCGTs have lower incentives for commitment, which decreases the committed balancing capacity and increases the value of the slow adder.

This last point highlights a fundamental difference between the variations in terms of distribution of imbalance increments

			Fast reserve adder	Slow reserve adder
8300	Pre-Acti.	Ind.	5.78	0.25
		Corr.	2.86	0.36
	Post-Act.	Ind.	5.78	0.14
		Corr.	2.74	0.30
13500	Pre-Act.	Ind.	6.50	0.37
		Corr.	3.28	0.56
	Post-Act.	Ind.	6.20	0.21
		Corr.	2.92	0.32

Fig. 2. Adder payoff as a function of the risk aversion of the agents.

versus the variations of the VOLL. The independent and correlated variants only impact the 7.5-minute ORDC and increase or decrease the incentives for committing CCGTs, while keeping the slow reserve demand constant. In comparison, variations of the VOLL impact both the 7.5-minute and 15-minute ORDCs.

Fig. 2 provides an indication about the persistence of the price signal generated by the ORDC in terms of profitability for owners of flexible assets. The figure compares the price signal obtained by 4 variants, beginning with the most conservative variant that produces the highest adder (13500/Post-activation/Independent) and modifying each of the design parameters in turn. The y-axis displays the measure of the adder under the metric of conditional value at risk as a function of the risk aversion of the agents on the x-axis. Depending on the risk aversion α of an agent, the agent will only consider the $100 - \alpha$ worst adders for computing its expected payoffs from the adder. The risk aversion can range from 0% to 100%, where 0% is a completely risk-neutral agent and 100% is a completely risk-averse one.

We observe a notable drop in the value of the payoff curve for low values of the x axis, which corresponds to the impact of a very high adder resulting from very stressed conditions in the system. These highly stressed conditions constitute less than 1% of the total possible outcomes in the system. It is possible to assess the quality of the signal produced by a variant by analysing the persistence of the adder when the risk aversion increases.

In Fig. 2 we observe that the correlated variant is the least persistent by a wide margin. The variants related to the value of lost load and the pre/post-activation capacity produce similar levels of persistence. Note that, for these variants, the decrease can be considered constant until a risk aversion level of 7.5%, which indicates a mean adder that is generated by the repetition of a large number of occurrences of small adders in the market, which is desirable from the perspective of mitigating investment risk.

Fig. 3 presents the mean fast adder per day for 2018. It shows that the mean price per day is between 0 and 10 €/MWh for the majority of the time, while during approximately 50 days the average adder is higher than 10 €/MWh.
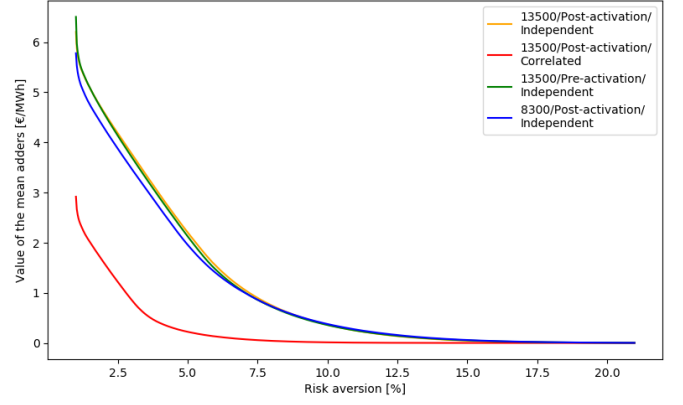
C. Sensitivity Analysis for the Variation of the Availability of Slow Balancing Capacity for the 7.5-Minute ORDC

The eligibility of slow balancing capacity for the 7.5-minute ORDC is an important determinant for the remuneration of flexible assets. In principle, the eligibility of these resources should be plant-dependent and should reflect as accurately as possible their reactivity. For reasons of simplicity, the current Belgian scarcity pricing proposal only assumes a generic value for the availability. ELIA [15] assumes an availability of 50%, and our analysis considers availabilities ranging from 0% to 28%.

Given an availability ρ, the parameters $R_g^{SU,0}$ in Eq. (47) and $R_g^{NS,F}$ in Eq. (26) for the emergency generators and demand response are modified as follows:

$$R_g^{SU,0} = R_g^{NS,F} = \rho \cdot R_g^{NS,S}. \tag{51}$$

The effects of modifying the availability on the adder are two-fold, and can be observed in Table IV. Increasing ρ (i) reduces notably the level of the fast adder by increasing the fast balancing capacity pool, and (ii) increases marginally the level of the slow reserve adder. Increasing the availability of mFRR for covering the demand of the 7.5-minute ORDC reduces the need for aFRR from CCGTs, and has a direct effect on their commitment. This compresses the committed balancing capacity, which in turn increases the level of the slow adder.

VI. CONCLUSION

We develop a detailed unit commitment and economic dispatch simulation model of the Belgian power system in order to analyze the effect of different design choices for Operating Reserve Demand Curves on the cost of system operation and the price of aFRR and mFRR capacity. Our simulator attempts to emulate a best-case, fully coordinated operation of the system from the day ahead to real time. We propose four modules that are interleaved and implemented as a rolling horizon optimization.

The precision of our model allows us to account for the tension between incurring fixed costs for committing flexible resources that can allow the system to operate reliably in real time, versus running the risk of shedding load.
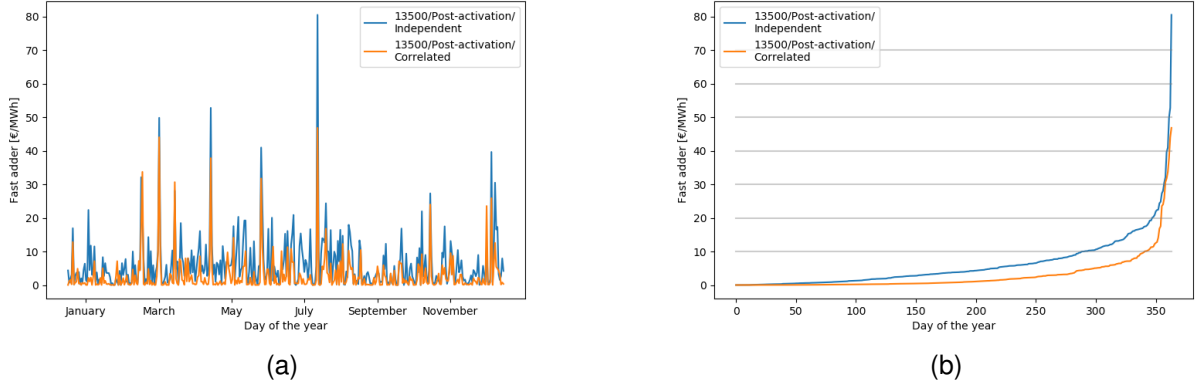
Fig. 3. (a) Yearly distribution and (b) cumulative distribution of the mean fast reserve adder per day [€/MWh] for 2018.

TABLE IV
FAST AND SLOW RESERVE ADDER IN €/MWH AS A FUNCTION OF ρ, THE AVAILABILITY OF THE SLOW BALANCING CAPACITY FOR COVERING THE DEMAND OF THE 7.5-MINUTE ORDC.

			Fast reserve adder			Slow reserve adder		
	ρ		0%	28%	50%	0%	28%	50%
8300	Pre-Acti.	Ind.	14.65	5.78	1.57	0.12	0.25	0.33
		Corr.	12.88	2.86	0.81	0.19	0.36	0.54
	Post-Act.	Ind.	14.62	5.78	1.51	0.08	0.14	0.29
		Corr.	13.33	2.74	0.74	0.14	0.30	0.48
13500	Pre-Act.	Ind.	14.76	6.50	1.66	0.25	0.37	0.32
		Corr.	12.92	3.28	0.90	0.27	0.56	0.62
	Post-Act.	Ind.	14.91	6.20	1.55	0.09	0.21	0.25
		Corr.	13.12	2.92	0.92	0.17	0.32	0.62

We validate our model against historically observed data of the Belgian market for 2018. We then perform a case study on the impact of ORDCs on scarcity prices and system costs for 2018. We also perform a sensitivity analysis on the extent to which mFRR reserves are assumed to contribute towards satisfying the demand for 7.5-minute reserves.

The main findings of our analysis can be summarized as follows:

1) The total flexible operating cost for a day is stable, regardless of the chosen ORDC variant. It is also stable for the specific generation pool of Belgium that is investigated in our work.
2) The fast adder varies from 2.8 €/MWh to 6.5 €/MWh in the reference scenario. The main driver of the price is the assumption related to the distribution of the 7.5-minute imbalance increments, followed by the value of lost load.
3) The level of the fast adder is sensitive to assumptions about what resources can contribute towards covering the demand of the 7.5-minute ORDC. Note that this sensitivity was already reported in [15].

In future work, we are interested in developing a Monte Carlo simulation model for the Belgian system which draws samples of system uncertainty, instead of relying on historical data. This would allow us to enhance the statistical reliability of our results, by exposing the system to multiple years of hypothetical operation.

APPENDIX
REFERENCES

[1] S. Stoft, "Power System Economics: Designing Markets for Electricity," *undefined*, 2002. [Online]. Available: https://www.semanticscholar.org/paper/Power-System-Economics%3A-Designing-Markets-for-Stoft/8ed77a99087bce18c09f8b1f6b4d7f1276622206
[2] W. W. Hogan, "On an "Energy Only" electricity market design for resource adequacy," p. 39, Sep. 2005.
[3] ——, "Electricity Scarcity Pricing Through Operating Reserves," *Economics of Energy & Environmental Policy*, vol. Volume 2, no. Number 2, 2013. [Online]. Available: https://ideas.repec.org/a/aen/eeepjl/2_2_a04.html
[4] NYISO, "Ancillary Services Shortage Pricing," Tech. Rep., Dec. 2019.
[5] E. a. I. S. Department for Business, "GB Implementat!ion Plan," Department for Business, Energy and Industrial Strategy, Tech. Rep., 2020.
[6] SEM, "Discussion Paper and Call for Evidence on Scarcity Pricing and Demand Response in the SEM," Tech. Rep., May 2021.
[7] ——, "Training Modules, Chapter 10: Administered Scarcity Pricing and Reserve Scarcity Pricing."
[8] Polskie Sieci Elektroenergetyczne, "KONCEPCJA zmian zasad unkcjonowania rynku bilansujacego w Polsce," Warsaw, Tech. Rep., Nov. 2019.
[9] A. Papavasiliou, Y. Smeers, and G. Bertrand, "Remuneration of Flexibility using Operating Reserve Demand Curves: A Case Study of Belgium," *The Energy Journal*, vol. 38, no. 01, Sep. 2017. [Online]. Available: http://www.iaee.org/en/publications/ejarticle.aspx?id=3004
[10] ——, "An Extended Analysis on the Remuneration of Capacity under Scarcity Conditions," *Economics of Energy & Environmental Policy*, vol. 7, no. 2, Apr. 2018. [Online]. Available: http://www.iaee.org/en/publications/eeeparticle.aspx?id=232
[11] A. Papavasiliou, Y. Smeers, and G. de Maere d'Aertrycke, "Market Design Considerations for Scarcity Pricing: A Stochastic Equilibrium Framework," *The Energy Journal*, vol. 42, no. 01, Sep. 2021. [Online]. Available: http://www.iaee.org/en/publications/ejarticle.aspx?id=3734
[12] A. Papavasiliou and G. Bertrand, "Market Design Option for Scarcity Pricing in European Balancing Markets," 2020.
[13] A. Papavasiliou, "Scarcity pricing and the missing European market for real-time reserve capacity," *The Electricity Journal*, vol. 33, no. 10, p. 106863, Dec. 2020. [Online]. Available: https://www.sciencedirect.com/science/article/pii/S104061902030155X

[14] J. Zarnikau, S. Zhu, C. K. Woo, and C. H. Tsai, "Texas's operating reserve demand curve's generation investment incentive," *Energy Policy*, vol. 137, no. C, 2020, publisher: Elsevier. [Online]. Available: https://ideas.repec.org/a/eee/enepol/v137y2020ics030142151930730x.html

[15] ELIA, "Study report on Scarcity Pricing in the context of the 2018 discretionary incentives," Tech. Rep., Oct. 2018.

[16] Z. Zhou and A. Botterud, "Dynamic Scheduling of Operating Reserves in Co-Optimized Electricity Markets With Wind Power," *IEEE Transactions on Power Systems*, vol. 29, no. 1, pp. 160–171, Jan. 2014, conference Name: IEEE Transactions on Power Systems.

[17] L. Lavin, S. Murphy, B. Sergi, and J. Apt, "Dynamic operating reserve procurement improves scarcity pricing in PJM," *Energy Policy*, vol. 147, p. 111857, Dec. 2020. [Online]. Available: https://www.sciencedirect.com/science/article/pii/S0301421520305747

[18] H. Simao, W. Powell, C. Archer, and W. Kempton, "The challenge of integrating offshore wind power in the U.S. electric grid. Part II: Simulation of electricity market operations," *Renewable Energy*, vol. 103, pp. 418–431, Apr. 2017. [Online]. Available: https://www.sciencedirect.com/science/article/abs/pii/S0960148116310333

[19] E. A. Bakirtzis, C. K. Simoglou, P. N. Biskas, D. P. Labridis, and A. G. Bakirtzis, "Comparison of advanced power system operations models for large-scale renewable integration," *Electric Power Systems Research*, vol. 128, pp. 90–99, Nov. 2015. [Online]. Available: https://www.sciencedirect.com/science/article/pii/S0378779615002011

[20] W. W. Hogan and S. L. Pope, "PJM Reserve Markets: Operating Reserve Demand Curve Enhancements," p. 87, Mar. 2019.

[21] A. Papavasiliou, Y. Smeers, and G. de Maere d'Aertrycke, "Study on the general design of a mechanism for the remuneration of reserves in scarcity situations," p. 90, Jun. 2019.

[22] H. Transmission, Amrpion, E. S. Operator, T. TSO, and TransnetBW, "Potential Cross-Border Balancing Cooperation Between the Belgian, Dutch and German Electricity Transimission System Operators," Tech. Rep., Oct. 2014.

[23] W. W. Hogan and S. L. Pope, "Real-Time Co-Optimization with the ERCOT ORDC," Mar. 2020.

[24] D. Devogelaer, "Increasing interconnections: to build or not to build, that is (one of) the question(s)," Federal Planning Bureau, Tech. Rep., Sep. 2017.

[25] CREG, "Décision 1806," Tech. Rep., Sep. 2018. [Online]. Available: https://www.creg.be/sites/default/files/assets/Publications/Decisions/B1806FR.pdf

[26] ELIA, "Installed Capacity By Units 2018." [Online]. Available: https://www.elia.be/fr/donnees-de-reseau/data-download-page

[27] ——, "Adequacy and flexibility study for Belgium 2020-2030," ELIA, Tech. Rep., 2019.

[28] ——, "Data Download Page," May 2021. [Online]. Available: https://www.elia.be/fr/donnees-de-reseau/data-download-page

[29] ENTSO-E, "ENTSO-E Transparency Platform," May 2021. [Online]. Available: https://transparency.entsoe.eu/